Published in final edited form as:
Cell Rep. 2014 October 23; 9(2): 591–604. doi:10.1016/j.celrep.2014.09.032.

Non-classical Ly6C⁻ monocytes drive the development of inflammatory arthritis in mice

Alexander V Misharin[1], **Carla M Cuda**[1], **Rana Saber**[1], **Jason D Turner**[2], **Angelica K Gierut**[1], **G. Kenneth Haines**[3], **Sergejs Berdnikovs**[4], **Andrew Filer**[2], **Andrew R Clark**[2], **Christopher D Buckley**[2], **Gökhan M Mutlu**[5], **G.R. Scott Budinger**[6], and **Harris Perlman**[1,7]

[1]Division of Rheumatology, Feinberg School of Medicine, Northwestern University, Chicago, IL, USA

[2]Rheumatology Research Group, College of Medical and Dental Sciences, The University of Birmingham, Birmingham, UK

[3]Department of Pathology, Yale University, School of Medicine, New Haven, CT, USA

[4]Division of Allergy and Immunology, Feinberg School of Medicine, Northwestern University, Chicago, IL, USA

[5]Section of Pulmonary and Critical Care, Department of Medicine, University of Chicago, Chicago, IL, USA

[6]Division of Pulmonary and Critical Care, Feinberg School of Medicine, Northwestern University, Chicago, IL, USA

Summary

Different subsets and/or polarized phenotypes of monocytes and macrophages may play distinct roles during the development and resolution of inflammation. Here, we demonstrate in a murine model of rheumatoid arthritis that non-classical Ly6C⁻ monocytes are required for the initiation and progression of sterile joint inflammation. Moreover, non-classical Ly6C⁻ monocytes differentiate into inflammatory macrophages (M1), which drive disease pathogenesis and display plasticity during the resolution phase. During the development of arthritis, these cells polarize toward an alternatively activated phenotype (M2), promoting the resolution of joint inflammation. The influx of Ly6C⁻ monocytes and their subsequent classical and then alternative activation occurs without changes in synovial tissue-resident macrophages, which express markers of M2 polarization throughout the course of the arthritis and attenuate joint inflammation during the initiation phase. These data suggest that circulating Ly6C⁻ monocytes recruited to the joint upon injury orchestrate the development and resolution of autoimmune joint inflammation.

[7]Corresponding author: Harris Perlman, PhD, 240 E Huron st. M300, Division of Rheumatology, Feinberg School of Medicine, Northwestern University, Chicago, IL, USA, Phone: 312-503-1955, Fax: 312-503-0994, h-perlman@northwestern.edu.

Additional Materials and Methods can be found in Supplemental Materials.

Introduction

Our understanding of the mononuclear phagocyte system in the initiation and resolution of inflammation has been significantly revised over the past years, in part due to discovery of heterogeneity of peripheral blood monocytes and tissue macrophages (Davies et al., 2013a; Ginhoux and Jung, 2014). Peripheral blood monocytes are subclassified into three different populations based on expression of cell surface molecules and functions (Ziegler-Heitbrock et al., 2010). In humans, these populations correspond to $CD14^{++}CD16^{-}$ (classical monocytes), $CD14^{+}CD16^{+}$ (intermediate monocytes) and $CD14^{+}CD16^{++}$ (non-classical monocytes) and in mice the equivalent populations are $Ly6C^{+}CD62L^{+}CD43^{-}CCR2^{+}$ (classical monocytes), $Ly6C^{int}CD62L^{-}CD43^{+}CCR2^{-}$ (intermediate monocytes), and $Ly6C^{-}CD62L^{-}CD43^{+}CCR2^{-}$ (non-classical monocytes). An emerging literature suggests a previously unrecognized role for non-classical $Ly6C^{-}$ monocytes during tissue injury. These cells patrol the luminal side of the endothelium and extravasate in response to both septic and aseptic tissue injury (Auffray et al., 2007), and recent work suggests that these cells may serve as precursors for alternatively activated macrophages (Auffray et al., 2009; Nahrendorf et al., 2007), playing a protective or anti-inflammatory role during tissue injury (Hamers et al., 2012; Hanna et al., 2012). However, the relative contribution of classical $Ly6C^{+}$ compared with non-classical $Ly6C^{-}$ monocytes to tissue injury and repair is incompletely understood.

Another major component of the mononuclear phagocyte system is represented by tissue-resident macrophages. Classic work by van Furth identified bone marrow-derived monocytes as precursors to tissue macrophages (van Furth and Cohn, 1968). However, recent studies showed that many tissue macrophages such as microglia in the brain, peritoneal macrophages and Kupffer cells in the liver, originate from yolk sac or fetal liver progenitors (Ginhoux et al., 2010; Schulz et al., 2012; Yona et al., 2013). These tissue-resident macrophages are long-lived and self-renewing via *in situ* proliferation even in the absence of recruitment of circulating monocytes (Davies et al., 2011; Hashimoto et al., 2013; Jenkins et al., 2011), and have a gene expression profile specific to their anatomical localization and microenvironment (Gautier et al., 2012). In adult animals, the macrophage population in the lung, peritoneal cavity and spleen is more heterogeneous, with the addition of bone marrow-derived macrophages during steady state and inflammatory conditions (Davies et al., 2013b; Yona et al., 2013). The pro- and anti-inflammatory properties of tissue-resident macrophages have been primarily studied as a single population in the context of inflammation caused by microbes or parasites (Cailhier et al., 2006; Davies et al., 2011; Jenkins et al., 2011; Maus et al., 2002). Moreover, the roles of tissue-resident macrophages during sterile inflammation are unknown and the relative contributions of tissue resident or monocyte-derived macrophages in any models of inflammation are largely unexplored.

Both tissue-resident and bone marrow-derived macrophages exhibit significant functional heterogeneity and may differentiate or be polarized into one of two main macrophage subtypes: classically activated, M1 (pro-inflammatory), and alternatively activated, M2 (anti-inflammatory/resolution phase) macrophages (Lech and Anders, 2013; Sica and Mantovani, 2012). While some studies suggest that alternatively, anti-inflammatory

macrophages may originate from a new wave of monocytes entering into tissues during the resolution of inflammation (Nahrendorf et al., 2007; Shechter et al., 2009; Shechter et al., 2013), it is still not known if during disease pathogenesis bone marrow-derived classically activated macrophages can exhibit plasticity and switch their phenotype towards an alternatively activated one *in situ*.

Rheumatoid arthritis (RA) is a chronic autoimmune disease affecting up to 1% of the world's population (Helmick et al., 2008), which makes it one of the most prevalent autoimmune conditions. During RA, the dysregulation of the immune system leads to destruction and deformation of the joint, resulting in chronic pain, severe disability and increased mortality. Circulating monocytes in patients with RA are known to be activated (Kawanaka et al., 2002; Kinne et al., 2007; Stuhlmuller et al., 2000; Torsteinsdottir et al., 1999), and the number of macrophages in the synovium correlates with joint damage (Mulherin et al., 1996) and clinical response to therapy (Haringman et al., 2005). Murine models of RA represent a clinically relevant system for deciphering the role of monocytes and macrophages in the pathogenesis of sterile chronic autoimmune inflammation (Vincent et al., 2012).

Here, we used a mouse model of immune-complex, sterile, inflammatory arthritis to uncover novel roles for monocyte subsets and macrophages during distinct phases of disease development. We demonstrate that circulating Ly6C$^-$ monocytes are recruited to the joint during the effector phase of arthritis and differentiate into classically activated macrophages, which drive the development of the joint pathology. However, as the arthritis progresses, these same classically activated macrophages change from a classically to an alternatively activated phenotype, which is necessary for the resolution of joint inflammation. This remarkable influx of Ly6C$^-$ monocytes and their dramatic changes in polarization occurred without significant changes in the number or phenotype of tissue-resident synovial macrophages. These findings suggest a new paradigm for understanding the pathogenesis of RA in which non-classical monocytes recruited to the joint exhibit remarkable phenotypic plasticity over the course of arthritis, promoting first tissue injury and then repair, overwhelming the constitutive anti-inflammatory effects of the tissue-resident macrophages.

Results

Differential role of monocyte subsets in the initiation of inflammatory arthritis

The temporal changes in monocyte populations in murine models of autoimmune arthritis and their contribution to important disease phenotypes are still unknown. Here we used a murine model of sterile inflammatory arthritis (K/BxN **s**erum **t**ransfer **i**nduced **a**rthritis, STIA), which models the effector phase of human RA, is independent of the adaptive immune response and consists of initiation, propagation and resolution phases (Monach et al., 2008). To deplete monocytes, we injected clodronate-loaded liposomes intravenously 24 hours prior to the induction of arthritis. Virtually all monocytes in the peripheral blood and the red pulp macrophages in spleen were depleted for 48–72 hours following the clodronate-loaded liposome treatment, while the number of circulating neutrophils and synovial macrophages was unchanged (Figure S1A). Monocyte depletion completely prevented the development of STIA (Figure 1A) and suppressed the recruitment of neutrophils to the joints

(Figure S1B). Additionally, treatment with clodronate-loaded liposomes at days 3 and 5 of STIA led to an abrupt end to the development of STIA (Figure 1B). Since recent studies suggested that the splenic pool of monocytes may also contribute to acute inflammation, we splenectomized mice and showed that there was no difference in ankle swelling or clinical scores between the groups following the induction of STIA (Figure S1C).

To address the contribution of $Ly6C^+$ monocytes to the initiation and development of STIA we depleted classical $Ly6C^+$ monocytes using anti-CCR2 antibody. While $Ly6C^+$ monocytes were dramatically reduced in the peripheral blood and spleen following injection of anti-CCR2 antibody (Figure S1D), the induction and development of STIA occurred normally (Figure S1E). Similarly $CCR2^{-/-}$ mice, which lack CCR2 on both classical and non-classical monocytes, were able to develop STIA and recruit both neutrophils and macrophages into the joint (Figure S1F).

Since tools for selective depletion of non-classical $Ly6C^-$ monocytes are not available, we developed novel approaches to investigate the role of this population in the initiation of STIA. First, we depleted monocytes using clodronate-loaded liposomes and STIA was induced at different stages of monocyte subset recovery. While non-classical $Ly6C^-$ monocytes failed to recover even 7 days after injection of clodronate-loaded liposomes, the total number of monocytes and neutrophils were similar to controls at 7 days following the injection of clodronate-loaded liposomes (Figure 1C and Figure S1G). The absence of $Ly6C^-$ monocytes was also associated with an inability to develop STIA (Figure 1D). Next, we treated mice with clodronate-loaded liposomes two days prior to the initiation of arthritis and classical $Ly6C^+$ or non-classical $Ly6C^-$ monocytes isolated from bone marrow were adoptively transferred immediately after initiation of STIA. Mice that received $Ly6C^-$ monocytes developed STIA at the same rate as control treated animals (Figure 1E); however, mice that received $Ly6C^+$ monocytes exhibited a marked delay in the development of STIA. These results likely reflect the conversion of classical $Ly6C^+$ monocytes into non-classical $Ly6C^-$ monocytes after adoptive transfer (Yona et al., 2013) or recovery of the depleted monocyte pool.

The normal adult mouse joint contains heterogeneous population of tissue-resident macrophages

To further explore the role of $Ly6C^-$ non-classical monocyte subsets in the development of inflammatory arthritis, we first examined the cellular composition of the murine joint in unchallenged, normal wild-type mice using multi-parameter flow cytometry (Figure 2A). After excluding doublets, dead cells, and non-hematopoietic cells, we identified myeloid cells as $CD11b^+$ and then excluded eosinophils (Siglec F^+), neutrophils ($Ly6G^+$) and $CD11b^+$ DCs ($CD11b^+CD11c^{high}$MHC II^+CD64^-). We then subdivided the remaining $CD11b^+$ cells into $Ly6C^+CD11b^+CD11c^-F4/80^{low}CD64^{int}$ cells (referred as $Ly6C^+CD64^{int}$ cells) and $CD11b^+CD11c^{int}F4/80^+CD64^+$ cells (macrophages). We further subclassified the macrophage population as MHC II^+ or MHC II^-, with the majority being MHC II^- macrophages (80–85%). Cytospin analysis (Figure 2B) revealed that MHC II^- macrophages were smaller (10.0±1.8 μM vs. 8.9±1.8 μM, correspondingly), had more condensed chromatin in the nuclei, and more granular cytoplasm as compared to MHC II^+

macrophages, which had brighter nuclei and large vacuoles in the cytoplasm. Additionally, both populations of macrophages had similar surface expression of classic macrophage markers, receptors involved in phagocytosis and uptake of apoptotic bodies with the exception of Tim-4 and CX_3CR1 (Figure S2A). Immunofluorescent microscopy confirmed that the MHC II^+ and MHC II^- macrophages were located within the synovial lining (Figure S2B). Further, human synovial CD68+ macrophages obtained from synovial biopsies in healthy volunteers or patients with RA were also heterogeneous with respect to HLA-DR and CD163 expression (Figure S2C).

To define the contribution of bone marrow-derived monocytes to the persistence of $Ly6C^+CD64^{int}$ cells and MHC II^- and MHC II^+ synovial macrophages, we generated bone marrow chimeras by irradiating CD45.1 hosts and transferring CD45.2 bone marrow cells. Almost 80% of the MHC II^- synovial macrophages were recipient origin even two months post transfer (Figure 2C). These data suggest that this population was radio-resistant, long lived and does not require a contribution from circulating monocytes. In contrast, $Ly6C^+CD64^{int}$ cells and MHC II^+ macrophages were rapidly replaced by donor cells, similar to other bone marrow-derived macrophages, such as pulmonary interstitial macrophages, small peritoneal macrophages and splenic monocytes (Figure S2D). We then analyzed ankles from $CCR2^{-/-}$ mice, which have a decreased number of monocytes in the circulation. In agreement with the bone marrow chimera data, $CCR2^{-/-}$ mice had reduced numbers of $Ly6C^+CD64^{int}$ cells, $CD11b^+$ DC and MHC II^+ macrophages, while the numbers of MHC II^- macrophages were not affected (Figure S2E). The number of synovial MHC II^-, but not MHC II^+ macrophages was dramatically decreased in the ankle joint (Figure 2D) from mice that lack M-CSF ($Csf1^{op}/Csf1^{op}$). Since previous studies have suggested that M-CSF-responsive macrophages are derived from the yolk sac or fetal progenitors (Ginhoux et al., 2010; Ginhoux and Jung, 2014; Lichanska et al., 1999), these data suggest that under steady state conditions majority MHC II^- macrophages represent true tissue-resident macrophages, while most of the MHC II^+ synovial macrophages originate from bone marrow. Furthermore, as the host's $Ly6C^+CD64^{int}$ cells were completely replaced in the bone marrow chimeras, decreased in $CCR2^{-/-}$ mice, and unaffected by the intravenous injection of clodronate-loaded liposomes in WT mice, the $Ly6C^+CD64^{int}$ cells likely represent classical $Ly6C^+$ monocytes, which extravasated into tissues for surveillance (Jakubzick et al., 2013).

Peripheral blood monocytes give rise to recruited macrophages during STIA

To better understand the contribution of monocytes throughout the initiation, sustainment and remission phases of STIA, we analyzed the cellular composition of mouse ankles during the course of STIA. All populations of myeloid cells expanded during the initiation and propagation phases of STIA (Figure 3A). Neutrophils were the predominant cell subset during the peak of STIA, however, their number rapidly declined during the resolution phase. Macrophage populations also changed over the course of STIA. The MHC II^+ subset prevailed during the propagation phase, while the MHC II^- subset became the predominant cell type during the resolution phase (Figure 3A). We then focused on the early events of STIA (Figure S3A) and found an increase in the number of MHC II^+ macrophages first evident at day 2 followed by an increase in the number of neutrophils at Day 3. These data

indicate that the influx of monocytes and their differentiation into macrophages precedes the recruitment of neutrophils.

To unravel the relationships between the monocyte/macrophage subsets in the arthritic joint (blood monocytes, tissue-resident macrophages and inflammatory macrophages), we performed a series of cell labeling studies. To discriminate between tissue-resident (CD45.2) and recruited cells (CD45.1), we generated bone marrow chimeras (CD45.1→CD45.2) but this time the ankles were shielded during irradiation (see Supplemental Methods). Mice were then pulsed with a single injection of EdU during different stages of STIA (D-1, D2, D6 and D9) and incorporation of EdU into donor cells (CD45.1) and host tissue-resident macrophages (CD45.2) was analyzed 24 hours later (D0, D3, D7 and D10) (Figure 3B). Within this time frame, only classical Ly6C$^+$ monocytes were labeled in peripheral blood (Figure S3B). The percentage of EdU$^+$Ly6C$^+$CD64^{int} cells (CD45.1) was similar to circulating monocytes (CD45.1) (Figure 3B). The percent of EdU$^+$ MHC II$^+$ bone marrow-derived macrophages (CD45.1) was higher compared to EdU$^+$ MHC II$^-$ macrophages (Figure 3B). After 48 hours (D2 of STIA), the percent EdU$^+$ donor monocytes (CD45.1) and Ly6C$^+$CD64^{int} CD45.1 cells decreased, while the percent of EdU+ bone marrow-derived macrophages (CD45.1) reciprocally increased (Figure S3C). We then investigated whether local proliferation of tissue-resident macrophages contributes to the increased number of macrophages during STIA. Tissue-resident macrophages (CD45.2) exhibited low levels of proliferation in the steady state (D0, 1.47±0.51%), which increased during the peak of arthritis (day 7, 3.10±0.54%, p=0.0198) and returned to baseline during the resolution of STIA (day 10, 1.68±1.49%, p=0.82). However, despite their ability to proliferate, the total number of tissue-resident macrophages (CD45.2) did not change during the course of STIA. Moreover, the ratio of recruited macrophages to tissue-resident macrophages ranged between 7:1 and 20:1 during STIA (Figure S3D). Taken together, these data suggest that monocyte recruitment and not local proliferation of tissue-resident macrophages contributes to increased number of macrophages during STIA and that the overwhelming majority of macrophages in the joint are derived from monocytes that extravasate during STIA.

Non-classical Ly6C$^-$ monocytes preferentially give rise to MHC II$^-$ macrophages during STIA

Since our data indicate that non-classical Ly6C$^-$ monocytes are required for STIA (Figure 1C–D), we examined whether they are recruited into arthritic joint. We labeled Ly6C$^-$ monocytes (Figure 3C) and tracked their fate upon induction of STIA (Figure 3D). There were no labeled Ly6C$^-$ monocytes in the joint in the non-arthritic mouse three days post labeling (T=0). In contrast, the labeled Ly6C$^-$ monocytes entered into arthritic joint and developed into both MHC II$^-$ (77%) and MHC II$^+$ (22%) synovial macrophages during STIA (Figure 3D). These data indicate that non-classical Ly6C$^-$ monocytes give rise to inflammatory macrophages in the context of STIA. To determine fate of synovial macrophages during STIA, we adoptively transferred MHC II$^+$ and MHC II$^-$ synovial macrophages sorted from ankles of day 3 STIA *Cx3cr1*$^{gfp/+}$ mice into the periarticular space of day 3 STIA CD45.1 mice (Figures S3E–F). Synovial macrophages exhibited plasticity in terms of MHC II expression as 50% of transferred MHC II$^+$ macrophages became MHC II$^-$ and almost 25% of transferred MHC II$^-$ macrophages were MHC II$^+$ between days 3 and

day 10 of STIA. In contrast, when we sorted and adoptively transferred MHC II^+ and MHC II^- macrophages from day 7 of STIA and followed them into the late-resolution phase (day 18), almost 100% of cells became MHC II^- (Figures S3G–H).

Tissue-resident macrophages attenuate the severity of STIA

To understand the roles played by tissue-resident (MHC II^-) and bone marrow-derived (MHC II^+) macrophages in the development of STIA, we selectively deleted these populations from the naïve joint prior to the development of STIA. To accomplish this, we took advantage of the CD11b-DTR system, in which monocytes and bone marrow-derived macrophages express the diphtheria toxin receptor (DTR) under the control of the CD11b promoter. We used these mice to create two groups of bone marrow chimeras: 1) CD11b-DTR bone marrow (CD11b-DTR/CD45.2) into lethally irradiated CD45.1 recipients (CD11b-DTR→CD45.1); and 2) by CD45.1 bone marrow into CD11b-DTR/CD45.2 recipients (CD45.1→CD11b-DTR). Consistent with the wild-type chimeras (Figure 2C), more than 80% of the tissue-resident MHC II^- macrophages were of recipient origin, while the vast majority of the tissue-resident MHC II^+ macrophages were derived from the donor bone marrow (Figure 4A and C). We then treated CD11b-DTR→CD45.1 and CD45.1→CD11b-DTR mice with an intra-articular injection of low dose DT, which does not affect the circulating monocyte pool (Figure S4A) and then induced STIA 24 hours later. Loss of tissue-resident MHC II^+ macrophages in CD11b-DTR→CD45.1 mice had no effect (Figure 4B) on the course of STIA, while depletion of tissue-resident MHC II^- macrophages in CD45.1→CD11b-DTR mice led to increased arthritis (Figure 4D). To explore how tissue-resident macrophages might attenuate joint inflammation during STIA, we examined their phagocytic capacity *in vivo*. All MHC II^- macrophages phagocytized 2-MDa TRITC-labeled dextran, while only a portion (50%) of MHC II^+ macrophages were TRITC positive (Figure 4E). These data suggest that MHC II^- tissue-resident macrophages play important role in maintaining joint integrity and may limit the development of arthritis.

Recruited monocytes and inflammatory macrophages are required for the propagation phase in STIA

We have shown that non-classical $Ly6C^-$ monocytes are essential for the initiation and propagation of STIA and give rise to inflammatory macrophages. To investigate the role of these monocytes and bone marrow-derived macrophages during the effector phase of STIA we depleted them using by systemically administering DT to CD11b-DTR→CD45.1 chimeric mice. Peripheral blood monocytes and bone marrow-derived synovial macrophages were depleted after systemic treatment with DT (Figure 5A–B), while host MHC II^- tissue-resident macrophages (DTR^-) were insensitive to diphtheria toxin (DT) (Figure 5B). When we repeatedly treated CD11b-DTR→CD45.1 mice DT, the severity of arthritis as measured by ankle swelling and clinical scores was markedly decreased as compared to controls. The small amount of arthritis that developed in the CD11b-DTR→CD45.1 mice was associated with an increased number of neutrophils in the joint as compared to non-arthritic controls, but not macrophages (Figure 5D). Repeated administration of DT prevented the propagation phase (Figure 5D), which resulted in reduced histological scores of arthritis (Figure 5F–G). Additionally, the number of stromal ($CD45^-$) cells did not change throughout STIA (Figure 5E). To exclude a requirement for DCs in the development of STIA, we generated CD11c-

DTR→CD45.1 chimeric mice and subjected them to repeated administration of DT. Despite the fact that CD11b$^+$ DCs were deleted (Figure S4B), DT-treated mice exhibited similar levels of arthritis as compared to control mice (Figure S4C).

Recruited tissue macrophages but not blood monocytes are required for the resolution of STIA

Recent findings suggest that resolution of sterile inflammation may require recruitment of monocytes into tissues (Nahrendorf et al., 2007; Soehnlein and Lindbom, 2010). However, when we depleted blood monocytes at the peak of arthritis using intravenous injection of clodronate-loaded liposomes, the resolution of arthritis was unchanged (Figure 6A). In contrast, when we depleted both blood monocytes and recruited macrophages using systemic treatment of chimeric CD11b-DTR→CD45.1 mice with DT at the peak of arthritis, the resolution of arthritis was delayed as evidenced by sustained elevations in the histopathological scores for pannus, cartilage destruction and bone erosion relative to untreated mice (Figure 6B–E).

Synovial macrophages are reprogramed from inflammatory towards a resolution phenotype

Our data suggest that the same population of macrophages responsible for the development of arthritis also participated in its resolution. Macrophages may be polarized to a particular phenotype that is dependent on the environmental milieu, therefore, we examined whether synovial macrophages undergo a change in phenotype from classically activated M1 macrophages that drive destruction of the joint to alternatively activated M2 macrophages that are necessary for healing. Polarization of synovial macrophages in the naïve joint (D0) during the peak of STIA (D7) and during the resolution phase of STIA (D14) was assessed on sorted MHC II$^+$ and MHC II$^-$ synovial macrophages, which were analyzed for gene expression using a custom QuantiGene 2.0 panel (Table S4). Among the 52 genes included into the panel, 46 were differentially expressed between macrophage subsets according to selected criteria (differentially expressed in at least one two-group comparison, FDR-corrected q-value <0.001) (Table S5). Principal component analysis revealed that MHC II$^-$ and MHC II$^+$ macrophages in the naïve joint (D0) clustered separately from each other along PC2 axis, which is in agreement with differential origin of these populations (tissue-resident vs. bone marrow-derived) (Figure 7A and 7B). Twenty-three genes were differentially expressed between MHC II$^+$ and MHC II$^-$ macrophages in the steady state (D0) (Table S5), including *Timd4*, which is in agreement with data obtained via flow cytometry (Figure S2A). Further, the MHC II$^+$ and MHC II$^-$ macrophages recruited into the joint during STIA (D7 and D14) also clustered together. We then selectively compared the polarization profiles of synovial macrophages at the peak of STIA and during its resolution with MHC II$^+$ D0 macrophages, which are bone marrow-derived and therefore, more closely resemble macrophages recruited during STIA. At both the peak of STIA (Day 7) and during the resolution of STIA (Day 14), both MHC II$^+$ and MHC II$^-$ macrophages exhibited an enhanced M1 and intermediate M2 polarization profile compared with MHC II$^+$ macrophages at D0. These changes included increased expression of several M1 genes (*Nfkb1*, *Il1b*, *Cd80*, *Il12b* and *Fcrg1*) and some M2 genes (*Pparg*, *Tnfsf14*, *Il1rn*, *Tgm2*, *Chi3l3* and *Arg1*), with reduced expression of other M2 genes (*Timd4*, *Relma*, *Irf4*, *Cd36*,

Cxcl13, *Ccl17*, *Shpk*, *Nr4a1*, *Mrc1*). Interestingly, the expression of *Mertk*, which is involved in uptake of apoptotic cells, was increased in both MHC II^+ and MHC II^- macrophages during the resolution of STIA, but not at its peak.

We then compared the gene expression of MHC II^+ and MHC II^- macrophage populations at the peak (D7) of STIA. MHC II^+ macrophages expressed more M1-associated genes (*Il1b*, *Il12b*, *CD80*, *CD86*) and some M2-associated genes (*Pparg*, *Il1rn*, *Kdm6b*, *Tnfsf14*, *Socs1*, *Il33*, *Ccl17*) compared to MHC II^- macrophages. However, the expression of several M2 associated genes was increased in the MHC II^- compared with MHC II^+ macrophages including *Timd4*, *Tfrc*, *CD36*, *CD163*, *Cxcl13*, *Mertk*, and the hallmark gene of murine M2-activation – *Arg1*. The only M1-gene, which was expressed at higher levels in MHC II^- macrophages, was *Tnf*. A similar pattern was observed during the resolution phase of STIA (D14). Day 14 MHC II^+ macrophages expressed more M1- (*Il1b*, *Il6*, *Il12b*, *CD86*) and some M2-genes (*Retnla*, *Pparg*, *Il1rn*, *Kdm6b*, *Tnfsf14*, *Socs1*, *Il33*, *Ccl17*, *Irf4*, *Hbegf*, *Nr4a1*, *Il10*, *Mrc1*) while MHC II^- macrophages expressed higher levels of M2-genes (*Timd4*, *CD36*, *Cxcl13*, *Tgm2*, *Arg1*). Taken together, these data suggest that both MHC II^+ and MHC II^- macrophages exhibit mixed M1/M2 polarization during STIA. However, MHC II^- macrophages express more M2 genes throughout the course of STIA. Since many of the genes differentially expressed in MHC II^- macrophages are involved in uptake of apoptotic bodies and resolution of inflammation we analyzed expression of CD36 (Figure 7C), a member of class B scavenger receptor family involved in the uptake of apoptotic bodies (efferocytosis) and a marker of alternatively activated macrophages (Xiong et al., 2013). In agreement with the gene expression profiles, we found that only fraction MHC II^+ macrophages expressed CD36 during STIA, unlike MHC II^- macrophages, which uniformly expressed high levels of CD36. Taken together, these data and the fate mapping studies suggest that change in macrophage phenotype during STIA from MHC II^+ to MHC II^- is associated with transition from M1 to M2 phenotype.

Discussion

Synovial macrophages were discovered more than half a century ago and are known to be necessary for the development of arthritis (Barland et al., 1962), however, little is known about their origins and roles in maintenance of the normal joint or in the pathogenesis of RA. We used a strategy of depletion and selective rescue of non-classical $Ly6C^-$ monocytes to show they are both necessary and sufficient for the initiation of STIA. Our data are some of the first to show that non-classical $Ly6C^-$ monocytes can directly participate in tissue injury. Furthermore, our data suggest that the pathogenesis of autoimmune arthritis is distinct from other forms of tissue injury in which $Ly6C^+$ monocytes are preferentially recruited into inflamed tissues in a CCR2-dependent manner and give rise to inflammatory macrophages as has been described during bacterial infection (Auffray et al., 2007; Serbina et al., 2003) myocardial infarction (Nahrendorf et al., 2007), muscle injury (Arnold et al., 2007), and CNS injury (Shechter et al., 2013). Our data explain the previous observation that $CCR2^{-/-}$ mice, which have decreased numbers of classical $Ly6C^+$ monocytes, develop the same magnitude of STIA as controls and have a similar ability to recruit monocytes into the joint. We describe an approach that can be used to determine whether non-classical $Ly6C^-$ monocytes may contribute to tissue injury in other autoimmune models of

inflammation as has been suggested (Mildner et al., 2013; Soehnlein and Lindbom, 2010). For example, in a model of autoimmune kidney injury, Carlin et al. suggested that non-classical Ly6C$^-$ monocytes attract neutrophils in response to TLR7 stimulation and facilitate their extravasation into the tissue, however, they did not observe recruitment of non-classical Ly6C$^-$ monocytes, possibly due to the short duration of observation (Carlin et al., 2013). By selectively labeling only non-classical Ly6C$^-$ monocytes we were able to demonstrate that this monocyte subset is recruited into the joint during STIA, where they give rise to pro-inflammatory macrophages. Importantly, our strategy allowed us to follow the recruitment of non-classical Ly6C$^-$ monocytes into the joint in the presence of classical Ly6C$^+$ monocytes. If a similar distinct role for non-classical Ly6C$^-$ monocytes in the development of autoimmune inflammation in other models is confirmed, this would provide a new paradigm to understand the molecular basis of these diseases.

Currently, there are no strategies in mice to selectively deplete non-classical Ly6C$^-$ monocytes, however, their numbers are reduced in mice with deletions of CX_3CR1, NR4A1, or S1PR5 (Debien et al., 2013; Hanna et al., 2011; Landsman et al., 2009). While the impact of NR4A1 or S1PR5 deficiency on STIA has not been studied, mice lacking CX_3CR1 have been reported to develop less STIA (Jacobs et al., 2010). Our data in which even the adoptive transfer of a small number of non-classical Ly6C$^-$ monocytes was sufficient to induce STIA highlights the importance of this subset. Therefore, while our study does not dismiss important role of neutrophils and classical Ly6C$^+$ monocytes in STIA, it clearly demonstrates that non-classical Ly6C$^-$ monocytes are both necessary and sufficient for the initiation and propagation phases of arthritis.

The cellular composition of various macrophage populations in the naïve and inflamed joint has been largely unexplored. Flow cytometric analysis extending beyond assessment of CD11b or Gr-1 expression has only been reported in rats (Moghaddami et al., 2005a; Moghaddami et al., 2007; Moghaddami et al., 2005b) or synovial fluid of knee joints (Bruhns et al., 2003). None of these studies included techniques that determined the origin of synovial macrophages. Here, we generated bone marrow chimeric mice with selective shielding of the joint during irradiation to demonstrate that the naïve mouse joint contains a heterogeneous population of macrophages, namely tissue-resident and bone marrow-derived macrophages (Ginhoux and Jung, 2014; Hashimoto et al., 2013; Yona et al., 2013). In the naïve joint the vast majority of the tissue-resident synovial macrophages are MHC II$^-$, while the bone marrow-derived macrophages are mostly MHC II$^+$. Tissue-resident macrophages populate the synovial tissue early during embryonic development, and are derived from outside of the bone marrow via a process that requires M-CSF. If M-CSF is absent during early embryogenesis, the synovium is populated with bone marrow-derived macrophages, which may be recruited via IL-34, an alternative ligand for M-CSF-R (Wei et al., 2010). We found that depletion of tissue-resident MHC II$^-$ macrophages results in worsened STIA, suggesting these cells play an important role in maintaining tissue integrity and limiting inflammation (Lavin and Merad, 2013). We also show that tissue-resident macrophages exhibit a low level of proliferation during steady-state conditions and in inflammation. This local proliferation likely contributes to maintaining the population of tissue-resident macrophages during steady-state conditions, however, unlike other models of inflammation (Davies et al., 2011; Jenkins et al., 2011), it does not contribute to the increased number of

synovial macrophages during STIA, a large majority of which are monocyte-derived. This leaves open possibility that inefficient repair mediated by tissue-resident macrophages may play a role in chronic arthritis. Unlike tissue-resident macrophages, bone marrow-derived macrophages are short-lived and require constant influx of monocytes to maintain their population. Our short-term cell tracking studies suggest that bone marrow-derived monocytes do not contribute to the synovial macrophage population under steady-state conditions. However, in the absence of CCR2, $Ly6C^+$ monocytes can give rise to $Ly6C^+CD64^{int}$ cells, which may differentiate into macrophages. The $Ly6C^+CD64^{int}$ cells are not depleted after the systemic administration of clodronate-loaded liposomes, suggesting these cells may originate from extravasated tissue-surveying monocytes (Jakubzick et al., 2013).

Recently, macrophage polarization in health and disease has received a great deal of attention due to the therapeutic potential of altering macrophage phenotype. Macrophages may be readily manipulated *in vitro* to generate distinct classically activated/M1 or alternatively activated/M2 cells (Mosser and Edwards, 2008); however, their phenotypes *in vivo* may not be as straightforward (Sica and Mantovani, 2012; Xue et al., 2014). M1/M2 activation of synovial macrophages in STIA was dramatically different from M1 and M2 phenotypes obtained *in vitro* using LPS/INFγ or IL-4, correspondingly (data not shown). For example, iNOS, a hallmark of *in vitro* M1 activation, is not elevated at the peak of STIA. Similarly, *Mrc1* (CD206), *Retnla* (RELMα) and *Chi3l3* (Ym1) are not upregulated during the resolution phase. Instead, the resolution phase of STIA is associated with increased expression of genes involved in uptake of apoptotic debris and processing lipids, such as *Pparg* (PPARγ), *Mertk* (MerTK), *Tgm2* (Tgm2) and *Cd36* (CD36). The fact that subpopulations of synovial macrophages during the steady state and STIA exhibit mixed M1/M2 activation and differential expression of CD36 may suggest they are more heterogeneous than our current grouping based on expression of MHC II. Importantly, our findings of macrophage heterogeneity in mice are relevant to humans as we observed a similar phenomenon using synovial biopsies from healthy volunteers and patients with RA. New technologies, such as parallel single-cell RNA-Seq (Jaitin et al., 2014) has the potential to allow unbiased analysis of the change in macrophage phenotype using animal models of RA and synovial tissue.

While our labeling studies indicate that monocyte recruitment into the joints is continuous through all the phases of STIA, selective depletion of blood monocytes vs. recruited macrophages confirms that the recruited macrophages are necessary for the resolution of arthritis and healing of the joint. These data show that the same classically activated macrophages recruited during the development of STIA phase switch their phenotype and become wound healing macrophages, and, unlike in other models of inflammation, this process does not require the entrance of a second wave of monocytes into the tissue (Arnold et al., 2007; Nahrendorf et al., 2007; Shechter et al., 2009). This change in macrophage phenotype coincides with an upregulation of the molecules involved in efferocytosis and the rapid decrease in neutrophils from the joint, suggesting that apoptotic neutrophils into the joint during STIA may drive recruited macrophages towards a more M2 phenotype. This hypothesis is supported by findings in other models of tissue injury (Korns et al., 2011;

Soehnlein and Lindbom, 2010). While the systemic injection of apoptotic cells is not sufficient to prevent STIA (Gray et al., 2007), it is possible that phagocytosis of the apoptotic cells in the synovium may be more important for altering synovial macrophage phenotype than efferocytosis of apoptotic cells in the circulation. Consistent with this hypothesis, classically activated M1 macrophages recruited during early stages of STIA-mediated inflammation may efficiently clear apoptotic neutrophils (Korns et al., 2011).

In summary, we have identified a previously unrecognized role for non-classical Ly6C^{-} monocytes and tissue-resident macrophages in the development of autoimmune arthritis. Our data support a model in which Ly6C^{-} non-classical monocytes are recruited to the joint during inflammation where they are both required and sufficient for the development of arthritis. Over the course of SITA, these same recruited macrophages undergo a remarkable change in their pattern of gene expression, initially expressing express a complex set of both M1 and M2 genes followed by a shift toward a more M2 phenotype. This change in gene expression is accompanied by an alteration in function, as depletion of these macrophages at the peak of arthritis slows arthritis resolution. Throughout the course of STIA, tissue-resident synovial macrophages remain polarized toward a M2 phenotype and attenuate the severity of arthritis, however, their protective signals are likely overwhelmed by a relatively large influx of non-classical monocytes from the circulation. Whether this novel mechanism may be generalized to other forms of autoimmune inflammation in other tissues warrants further investigation. The approach we have developed demonstrates how a better longitudinal understanding of the roles of individual subsets of monocytes, tissue macrophages and neutrophils over the course of inflammation and its resolution can pave the way for improved strategies for targeting mononuclear phagocytes in autoimmune inflammation.

Experimental procedures

Mice

The following mouse strains were used: C57Bl/6, B6.SJL-*Ptprc*^{a} *Pepc*^{b}/BoyJ (CD45.1), *Cx3cr1*$^{gfp/+}$ (Jung et al., 2000), B6.Cg-*Gt(ROSA)26Sor*$^{tm6(CAG-ZsGreen1)Hze}$/J; B6;C3Fe a/a-Csf1^{op}/J (*Csf1*^{op}), B6.FVB-Tg(ITGAM-DTR/EGFP)34Lan/J (CD11b-DTR) and B6.FVB-Tg(Itgax-DTR/EGFP)57Lan/J (CD11c-DTR). All mice were purchased from the Jackson Laboratory and bred and housed at a barrier and specific pathogen-free facility at the Center for Comparative Medicine at Northwestern University (Chicago, IL, USA). Eight to ten -week-old mice were used for all experiments. All procedures were approved by the Institutional Animal Care and Use committee at Northwestern University. Generation of CD11b-DTR and CD11c-DTR bone marrow chimeras, diphtheria toxin treatment and monocyte depletion are described in Supplemental experimental procedures.

K/BxN Serum Transfer Induced Arthritis

Serum transfer arthritis was induced by intravenous injection of 75 μl of arthritogenic serum from 8-week-old progeny of KRN and NOD mice (K/BxN) mice (Monach et al., 2008). Change in ankle thickness was monitored using caliper (Fowler Tools of Canada). In addition, clinical score was assessed as a sum of the clinical score for each paw (0 – no

arthritis, 1 – mild arthritis, foot maintain V-shape, 2 – moderate arthritis, foot no longer maintain V-shape, 3 – severe arthritis). Each experiment was performed 2–5 times to confirm reproducibility. Whenever possible scoring was performed in a blinded manner. Histological and histopathological assessment of arthritis is described in Supplemental experimental procedures.

Tissue preparation and flow cytometry

Blood was collected into EDTA-containing tubes either via facial vein bleed (from live animals) or via cardiac puncture (from euthanized animals). Whole blood was stained with fluorochrome-conjugated antibodies and erythrocytes were then lysed using BD FACS lysing solution (BD Biosciences). Spleen was digested using mixture of Collagenase D and DNase I (both from Roche) in HBSS at 37°C for 30 min, and filtered through 40 μm nylon mesh. Erythrocytes were lysed using BD Pharm Lyse (BD Biosciences) and cells were counted using Countess automated cell counter (Invitrogen); dead cells were discriminated using trypan blue. For ankle analysis, mice were perfused through the left ventricle with 20 mL of HBSS. Ankles were cut 3 mm above the heel and skin from the feet was removed. To avoid contamination with the bone marrow, bone marrow cavity in the tibia was thoroughly flushed with HBSS, fingers were disarticulated by pulling with blunt forceps, and tibiotalar joint was opened via posterior access route to expose synovial lining. The foot was incubated in digestion buffer (2 mg/mL dispase II, 2 mg/mL collagenase D, and 1 mg/mL of DNase I in HBSS) for 60 min at 37°C. Cells released during the digestion were filtered through 40 μm nylon mesh, erythrocytes were lysed using BD Pharm Lyse (BD Biosciences) and cells were counted using Countess automated cell counter (Invitrogen); dead cells were discriminated using trypan blue. Cells were stained with live/dead Aqua (Invitrogen) or eFluor 506 (eBioscience) viability dyes, incubated with FcBlock (BD Bioscience) and stained with fluorochrome-conjugated antibodies (see Table S1 for the list of antibodies, clones, fluorochromes and manufacturers). Data were acquired on BD LSR II flow cytometer (BD Biosciences, San Jose, CA) (see Table S2 for instrument configuration). Compensation and analysis of the flow cytometry data were performed using FlowJo software (TreeStar, Ashland, OR). “Fluorescence minus one” controls were used when necessary to set up gates. Expression of the activation markers presented as median fluorescence intensity (MFI). Click-iT EdU Kit (Invitrogen) was used to assess the macrophage proliferation. Cell sorting was performed at University of Chicago Flow Cytometry core facility and at Northwestern University RLHCCC Flow Cytometry core facility on FACSAria III instrument (BD Biosciences, San Jose, CA) with the same configuration as LSR II. Cytospins were prepared from sorted cells and stained with Diff-Quik Stain Set (Siemens Healthcare, Malvern, PA). Microphotographs of the individual representative cells were taken on Nikon Eclipse TE2000E2 microscope, representative images of the individual cells were combined into one panel using Adobe Photoshop without any additional manipulations.

Analysis of macrophage polarization

Synovial macrophages from steady-state or STIA ankles were sorted using FACSAria III instrument, washed once and cell pellets were lysed directly in QuantiGene Cell Lysis Mixture. Gene expression profiles were determined using custom QuantiGene 2.0 assay

(panel #21522) (Affymetrix) on Luminex 200 instrument (Luminex Corporation), see Table S4 for the panel description. Data were normalized to expression of housekeeping genes and imported into Partek Genomics Suite V6.6 (PGS) software (Partek). Differentially expressed genes between the different groups of macrophages as well as transcripts with variable expression within the data set were calculated using one-way ANOVA. Differentially expressed genes were defined by a fold change greater than 1.4, and a false discovery rate (FDR)-corrected q-value <0.001 unless stated otherwise. Principle component analysis (PCA) using all transcripts was used for visualization of sample relationships. Hierarchical clustering of the differentially expressed genes was performed based on Euclidean algorithm for dissimilarity and average linkage method to determine distance between clusters.

Statistical analysis

In arthritis experiments, differences in ankle width and clinical score between the groups were assessed using 2-way ANOVA for repeated measurements with Bonferroni post-test to compare differences between the groups. For histopathological scores differences between groups were determined using Student's t-tests. All analyses were performed using GraphPad Prism version 5.00 (GraphPad Software, San Diego CA, USA). Data are shown as means ± SEM unless stated otherwise.

Supplementary Material

Refer to Web version on PubMed Central for supplementary material.

Acknowledgments

Northwestern University Cell Imaging Facility and Flow Cytometry Core Facility are supported by NCI Cancer Center Support Grant CA060553 awarded to the Robert H Lurie Comprehensive Cancer Center. This work was supported by NIH grants AR050250, AR054796, AI092490, and HL108795, Funds provided by Solovy/Arthritis Research Society, and Arthritis Research UK (grant 18547). We thank Dr. Steffen Jung for providing us with MC-21 antibody. We also thank Drs. Christian Stehlik, Navdeep Chandel and Richard M. Pope for their critical evaluation of the manuscript and valuable comments.

References

Arnold L, Henry A, Poron F, Baba-Amer Y, van Rooijen N, Plonquet A, Gherardi RK, Chazaud B. Inflammatory monocytes recruited after skeletal muscle injury switch into antiinflammatory macrophages to support myogenesis. J Exp Med. 2007; 204:1057–1069. [PubMed: 17485518]

Auffray C, Fogg D, Garfa M, Elain G, Join-Lambert O, Kayal S, Sarnacki S, Cumano A, Lauvau G, Geissmann F. Monitoring of blood vessels and tissues by a population of monocytes with patrolling behavior. Science. 2007; 317:666–670. [PubMed: 17673663]

Auffray C, Sieweke MH, Geissmann F. Blood monocytes: development, heterogeneity, and relationship with dendritic cells. Annu Rev Immunol. 2009; 27:669–692. [PubMed: 19132917]

Barland P, Novikoff AB, Hamerman D. Electron microscopy of the human synovial membrane. J Cell Biol. 1962; 14:207–220. [PubMed: 13865038]

Bruhns P, Samuelsson A, Pollard JW, Ravetch JV. Colony-stimulating factor-1-dependent macrophages are responsible for IVIG protection in antibody-induced autoimmune disease. Immunity. 2003; 18:573–581. [PubMed: 12705859]

Cailhier JF, Sawatzky DA, Kipari T, Houlberg K, Walbaum D, Watson S, Lang RA, Clay S, Kluth D, Savill J, Hughes J. Resident pleural macrophages are key orchestrators of neutrophil recruitment in pleural inflammation. Am J Respir Crit Care Med. 2006; 173:540–547. [PubMed: 16357332]

Carlin LM, Stamatiades EG, Auffray C, Hanna RN, Glover L, Vizcay-Barrena G, Hedrick CC, Cook HT, Diebold S, Geissmann F. Nr4a1-dependent Ly6C(low) monocytes monitor endothelial cells and orchestrate their disposal. Cell. 2013; 153:362–375. [PubMed: 23582326]

Davies LC, Jenkins SJ, Allen JE, Taylor PR. Tissue-resident macrophages. Nat Immunol. 2013a; 14:986–995. [PubMed: 24048120]

Davies LC, Rosas M, Jenkins SJ, Liao CT, Scurr MJ, Brombacher F, Fraser DJ, Allen JE, Jones SA, Taylor PR. Distinct bone marrow-derived and tissue-resident macrophage lineages proliferate at key stages during inflammation. Nat Commun. 2013b; 4:1886. [PubMed: 23695680]

Davies LC, Rosas M, Smith PJ, Fraser DJ, Jones SA, Taylor PR. A quantifiable proliferative burst of tissue macrophages restores homeostatic macrophage populations after acute inflammation. Eur J Immunol. 2011; 41:2155–2164. [PubMed: 21710478]

Debien E, Mayol K, Biajoux V, Daussy C, De Aguero MG, Taillardet M, Dagany N, Brinza L, Henry T, Dubois B, et al. S1PR5 is pivotal for the homeostasis of patrolling monocytes. Eur J Immunol. 2013; 43:1667–1675. [PubMed: 23519784]

Gautier EL, Shay T, Miller J, Greter M, Jakubzick C, Ivanov S, Helft J, Chow A, Elpek KG, Gordonov S, et al. Gene-expression profiles and transcriptional regulatory pathways that underlie the identity and diversity of mouse tissue macrophages. Nat Immunol. 2012; 13:1118–1128. [PubMed: 23023392]

Ginhoux F, Greter M, Leboeuf M, Nandi S, See P, Gokhan S, Mehler MF, Conway SJ, Ng LG, Stanley ER, et al. Fate mapping analysis reveals that adult microglia derive from primitive macrophages. Science. 2010; 330:841–845. [PubMed: 20966214]

Ginhoux F, Jung S. Monocytes and macrophages: developmental pathways and tissue homeostasis. Nat Rev Immunol. 2014; 14:392–404. [PubMed: 24854589]

Gray M, Miles K, Salter D, Gray D, Savill J. Apoptotic cells protect mice from autoimmune inflammation by the induction of regulatory B cells. Proc Natl Acad Sci U S A. 2007; 104:14080–14085. [PubMed: 17715067]

Hamers AA, Vos M, Rassam F, Marinkovic G, Kurakula K, van Gorp PJ, de Winther MP, Gijbels MJ, de Waard V, de Vries CJ. Bone marrow-specific deficiency of nuclear receptor Nur77 enhances atherosclerosis. Circ Res. 2012; 110:428–438. [PubMed: 22194623]

Hanna RN, Carlin LM, Hubbeling HG, Nackiewicz D, Green AM, Punt JA, Geissmann F, Hedrick CC. The transcription factor NR4A1 (Nur77) controls bone marrow differentiation and the survival of Ly6C- monocytes. Nat Immunol. 2011; 12:778–785. [PubMed: 21725321]

Hanna RN, Shaked I, Hubbeling HG, Punt JA, Wu R, Herrley E, Zaugg C, Pei H, Geissmann F, Ley K, Hedrick CC. NR4A1 (Nur77) deletion polarizes macrophages toward an inflammatory phenotype and increases atherosclerosis. Circ Res. 2012; 110:416–427. [PubMed: 22194622]

Haringman JJ, Gerlag DM, Zwinderman AH, Smeets TJ, Kraan MC, Baeten D, McInnes IB, Bresnihan B, Tak PP. Synovial tissue macrophages: a sensitive biomarker for response to treatment in patients with rheumatoid arthritis. Ann Rheum Dis. 2005; 64:834–838. [PubMed: 15576415]

Hashimoto D, Chow A, Noizat C, Teo P, Beasley MB, Leboeuf M, Becker CD, See P, Price J, Lucas D, et al. Tissue-resident macrophages self-maintain locally throughout adult life with minimal contribution from circulating monocytes. Immunity. 2013; 38:792–804. [PubMed: 23601688]

Helmick CG, Felson DT, Lawrence RC, Gabriel S, Hirsch R, Kwoh CK, Liang MH, Kremers HM, Mayes MD, Merkel PA, et al. Estimates of the prevalence of arthritis and other rheumatic conditions in the United States. Part I. Arthritis Rheum. 2008; 58:15–25. [PubMed: 18163481]

Jacobs JP, Ortiz-Lopez A, Campbell JJ, Gerard CJ, Mathis D, Benoist C. Deficiency of CXCR2, but not other chemokine receptors, attenuates autoantibody-mediated arthritis in a murine model. Arthritis Rheum. 2010; 62:1921–1932. [PubMed: 20506316]

Jaitin DA, Kenigsberg E, Keren-Shaul H, Elefant N, Paul F, Zaretsky I, Mildner A, Cohen N, Jung S, Tanay A, Amit I. Massively parallel single-cell RNA-seq for marker-free decomposition of tissues into cell types. Science. 2014; 343:776–779. [PubMed: 24531970]

Jakubzick C, Gautier EL, Gibbings SL, Sojka DK, Schlitzer A, Johnson TE, Ivanov S, Duan Q, Bala S, Condon T, et al. Minimal differentiation of classical monocytes as they survey steady-state tissues and transport antigen to lymph nodes. Immunity. 2013; 39:599–610. [PubMed: 24012416]

Jenkins SJ, Ruckerl D, Cook PC, Jones LH, Finkelman FD, van Rooijen N, MacDonald AS, Allen JE. Local macrophage proliferation, rather than recruitment from the blood, is a signature of TH2 inflammation. Science. 2011; 332:1284–1288. [PubMed: 21566158]

Jung S, Aliberti J, Graemmel P, Sunshine MJ, Kreutzberg GW, Sher A, Littman DR. Analysis of fractalkine receptor CX(3)CR1 function by targeted deletion and green fluorescent protein reporter gene insertion. Mol Cell Biol. 2000; 20:4106–4114. [PubMed: 10805752]

Kawanaka N, Yamamura M, Aita T, Morita Y, Okamoto A, Kawashima M, Iwahashi M, Ueno A, Ohmoto Y, Makino H. CD14+, CD16+ blood monocytes and joint inflammation in rheumatoid arthritis. Arthritis Rheum. 2002; 46:2578–2586. [PubMed: 12384915]

Kinne RW, Stuhlmuller B, Burmester GR. Cells of the synovium in rheumatoid arthritis. Macrophages. Arthritis Res Ther. 2007; 9:224. [PubMed: 18177511]

Korns D, Frasch SC, Fernandez-Boyanapalli R, Henson PM, Bratton DL. Modulation of macrophage efferocytosis in inflammation. Front Immunol. 2011; 2:57. [PubMed: 22566847]

Landsman L, Bar-On L, Zernecke A, Kim KW, Krauthgamer R, Shagdarsuren E, Lira SA, Weissman IL, Weber C, Jung S. CX3CR1 is required for monocyte homeostasis and atherogenesis by promoting cell survival. Blood. 2009; 113:963–972. [PubMed: 18971423]

Lavin Y, Merad M. Macrophages: gatekeepers of tissue integrity. Cancer Immunol Res. 2013; 1:201–209. [PubMed: 24777851]

Lech M, Anders HJ. Macrophages and fibrosis: How resident and infiltrating mononuclear phagocytes orchestrate all phases of tissue injury and repair. Biochim Biophys Acta. 2013; 1832:989–997. [PubMed: 23246690]

Lichanska AM, Browne CM, Henkel GW, Murphy KM, Ostrowski MC, McKercher SR, Maki RA, Hume DA. Differentiation of the mononuclear phagocyte system during mouse embryogenesis: the role of transcription factor PU.1. Blood. 1999; 94:127–138. [PubMed: 10381505]

Maus UA, Koay MA, Delbeck T, Mack M, Ermert M, Ermert L, Blackwell TS, Christman JW, Schlondorff D, Seeger W, Lohmeyer J. Role of resident alveolar macrophages in leukocyte traffic into the alveolar air space of intact mice. Am J Physiol Lung Cell Mol Physiol. 2002; 282:L1245–1252. [PubMed: 12003780]

Mildner A, Yona S, Jung S. A close encounter of the third kind: monocyte-derived cells. Adv Immunol. 2013; 120:69–103. [PubMed: 24070381]

Moghaddami M, Cleland LG, Mayrhofer G. MHC II+ CD45+ cells from synovium-rich tissues of normal rats: phenotype, comparison with macrophage and dendritic cell lineages and differentiation into mature dendritic cells in vitro. Int Immunol. 2005a; 17:1103–1115. [PubMed: 16030130]

Moghaddami M, Cleland LG, Radisic G, Mayrhofer G. Recruitment of dendritic cells and macrophages during T cell-mediated synovial inflammation. Arthritis Res Ther. 2007; 9:R120. [PubMed: 18028548]

Moghaddami M, Mayrhofer G, Cleland LG. MHC class II compartment, endocytosis and phagocytic activity of macrophages and putative dendritic cells isolated from normal tissues rich in synovium. Int Immunol. 2005b; 17:1117–1130. [PubMed: 16027140]

Monach PA, Mathis D, Benoist C. The K/BxN arthritis model. Curr Protoc Immunol. 2008; Chapter 15(Unit 15):22. [PubMed: 18491295]

Mosser DM, Edwards JP. Exploring the full spectrum of macrophage activation. Nat Rev Immunol. 2008; 8:958–969. [PubMed: 19029990]

Mulherin D, Fitzgerald O, Bresnihan B. Synovial tissue macrophage populations and articular damage in rheumatoid arthritis. Arthritis Rheum. 1996; 39:115–124. [PubMed: 8546720]

Nahrendorf M, Swirski FK, Aikawa E, Stangenberg L, Wurdinger T, Figueiredo JL, Libby P, Weissleder R, Pittet MJ. The healing myocardium sequentially mobilizes two monocyte subsets with divergent and complementary functions. J Exp Med. 2007; 204:3037–3047. [PubMed: 18025128]

Schulz C, Gomez Perdiguero E, Chorro L, Szabo-Rogers H, Cagnard N, Kierdorf K, Prinz M, Wu B, Jacobsen SE, Pollard JW, et al. A lineage of myeloid cells independent of Myb and hematopoietic stem cells. Science. 2012; 336:86–90. [PubMed: 22442384]

Serbina NV, Salazar-Mather TP, Biron CA, Kuziel WA, Pamer EG. TNF/iNOS-producing dendritic cells mediate innate immune defense against bacterial infection. Immunity. 2003; 19:59–70. [PubMed: 12871639]

Shechter R, London A, Varol C, Raposo C, Cusimano M, Yovel G, Rolls A, Mack M, Pluchino S, Martino G, et al. Infiltrating blood-derived macrophages are vital cells playing an anti-inflammatory role in recovery from spinal cord injury in mice. PLoS Med. 2009; 6:e1000113. [PubMed: 19636355]

Shechter R, Miller O, Yovel G, Rosenzweig N, London A, Ruckh J, Kim KW, Klein E, Kalchenko V, Bendel P, et al. Recruitment of beneficial M2 macrophages to injured spinal cord is orchestrated by remote brain choroid plexus. Immunity. 2013; 38:555–569. [PubMed: 23477737]

Sica A, Mantovani A. Macrophage plasticity and polarization: in vivo veritas. J Clin Invest. 2012; 122:787–795. [PubMed: 22378047]

Soehnlein O, Lindbom L. Phagocyte partnership during the onset and resolution of inflammation. Nat Rev Immunol. 2010; 10:427–439. [PubMed: 20498669]

Stuhlmuller B, Ungethum U, Scholze S, Martinez L, Backhaus M, Kraetsch HG, Kinne RW, Burmester GR. Identification of known and novel genes in activated monocytes from patients with rheumatoid arthritis. Arthritis Rheum. 2000; 43:775–790. [PubMed: 10765922]

Torsteinsdottir I, Arvidson NG, Hallgren R, Hakansson L. Monocyte activation in rheumatoid arthritis (RA): increased integrin, Fc gamma and complement receptor expression and the effect of glucocorticoids. Clin Exp Immunol. 1999; 115:554–560. [PubMed: 10193433]

van Furth R, Cohn ZA. The origin and kinetics of mononuclear phagocytes. J Exp Med. 1968; 128:415–435. [PubMed: 5666958]

Vincent TL, Williams RO, Maciewicz R, Silman A, Garside P. Arthritis Research U.K.a.m.w.g. Mapping pathogenesis of arthritis through small animal models. Rheumatology (Oxford). 2012; 51:1931–1941. [PubMed: 22427408]

Wei S, Nandi S, Chitu V, Yeung YG, Yu W, Huang M, Williams LT, Lin H, Stanley ER. Functional overlap but differential expression of CSF-1 and IL-34 in their CSF-1 receptor-mediated regulation of myeloid cells. J Leukoc Biol. 2010; 88:495–505. [PubMed: 20504948]

Xiong W, Frasch SC, Thomas SM, Bratton DL, Henson PM. Induction of TGF-beta1 Synthesis by Macrophages in Response to Apoptotic Cells Requires Activation of the Scavenger Receptor CD36. PLoS One. 2013; 8:e72772. [PubMed: 23936544]

Xue J, Schmidt SV, Sander J, Draffehn A, Krebs W, Quester I, De Nardo D, Gohel TD, Emde M, Schmidleithner L, et al. Transcriptome-based network analysis reveals a spectrum model of human macrophage activation. Immunity. 2014; 40:274–288. [PubMed: 24530056]

Yona S, Kim KW, Wolf Y, Mildner A, Varol D, Breker M, Strauss-Ayali D, Viukov S, Guilliams M, Misharin A, et al. Fate mapping reveals origins and dynamics of monocytes and tissue macrophages under homeostasis. Immunity. 2013; 38:79–91. [PubMed: 23273845]

Ziegler-Heitbrock L, Ancuta P, Crowe S, Dalod M, Grau V, Hart DN, Leenen PJ, Liu YJ, MacPherson G, Randolph GJ, et al. Nomenclature of monocytes and dendritic cells in blood. Blood. 2010; 116:e74–80. [PubMed: 20628149]

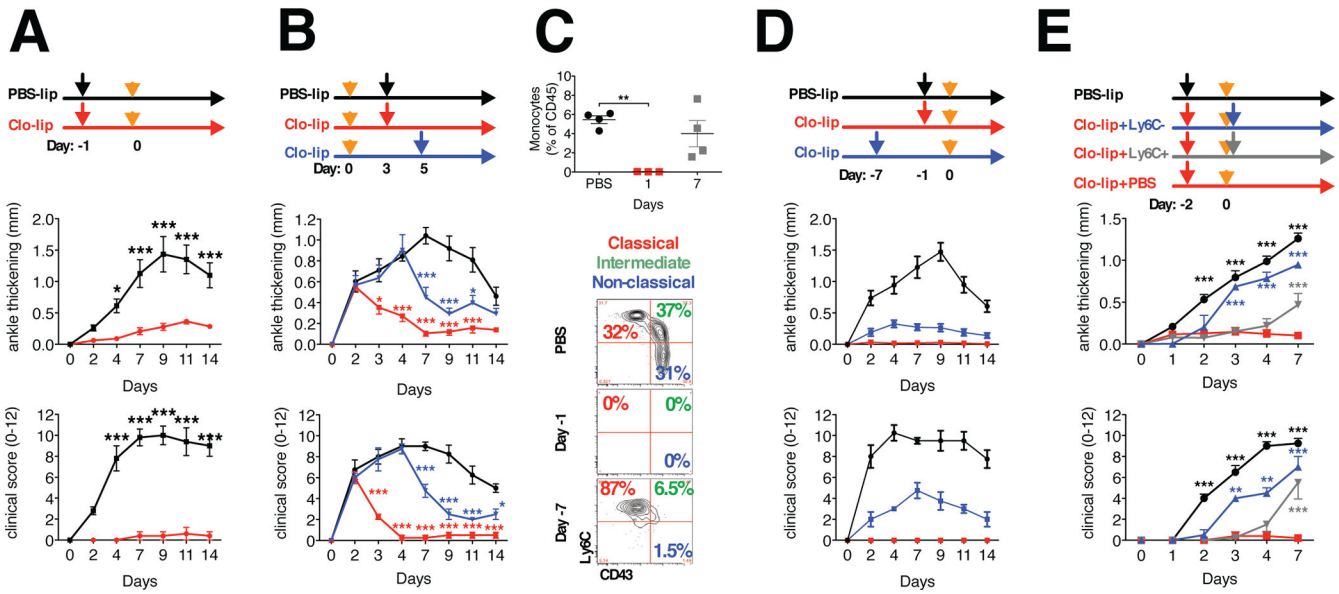

Figure 1. Role of monocytes in the initiation and development of STIA

A. Depletion of monocytes using clodronate-loaded liposomes prevents initiation and development of STIA (n = 5). Orange arrows indicate injection of K/BxN serum, black and red – PBS and clodronate-loaded liposomes correspondingly. B. Depletion of monocytes during development of STIA (n = 4) leads to its abrupt ending. Mice were treated with clodronate-loaded liposomes at indicated time points. Orange arrows indicate injection of K/BxN serum, black, blue and red – PBS and clodronate-loaded liposomes correspondingly. C–D. Absence of Ly6C$^-$ monocytes prevents STIA. Monocytes were depleted using clodronate-loaded liposomes. C. Representative contour plots gated on CD45$^+$CD115$^+$CD11b$^+$ blood cells (numbers represent percentages of the parent population). D. Representative arthritis scores (n = 4). E. Adoptive transfer of Ly6C$^-$ monocytes restores STIA. Monocytes were depleted with clodronate-loaded liposomes (red arrows) and 48 hours later 1×10^6 classical Ly6C$^+$ (n = 4) (grey arrow) or 0.5×10^6 non-classical Ly6C$^-$ (n = 2) (blue arrow) monocytes sorted from bone marrow or PBS (control) were transferred via intravenous injection, immediately following injection of K/BxN serum (orange arrows) to induce STIA. Another cohort of control mice was treated with PBS-loaded liposomes (n = 4) (black arrow). All data are represented as mean ± SEM. Differences between groups were compared using two-way ANOVA for repeated measurements, with Bonferroni post-test, * $p<0.05$, ** $p<0.01$, *** $p<0.001$.

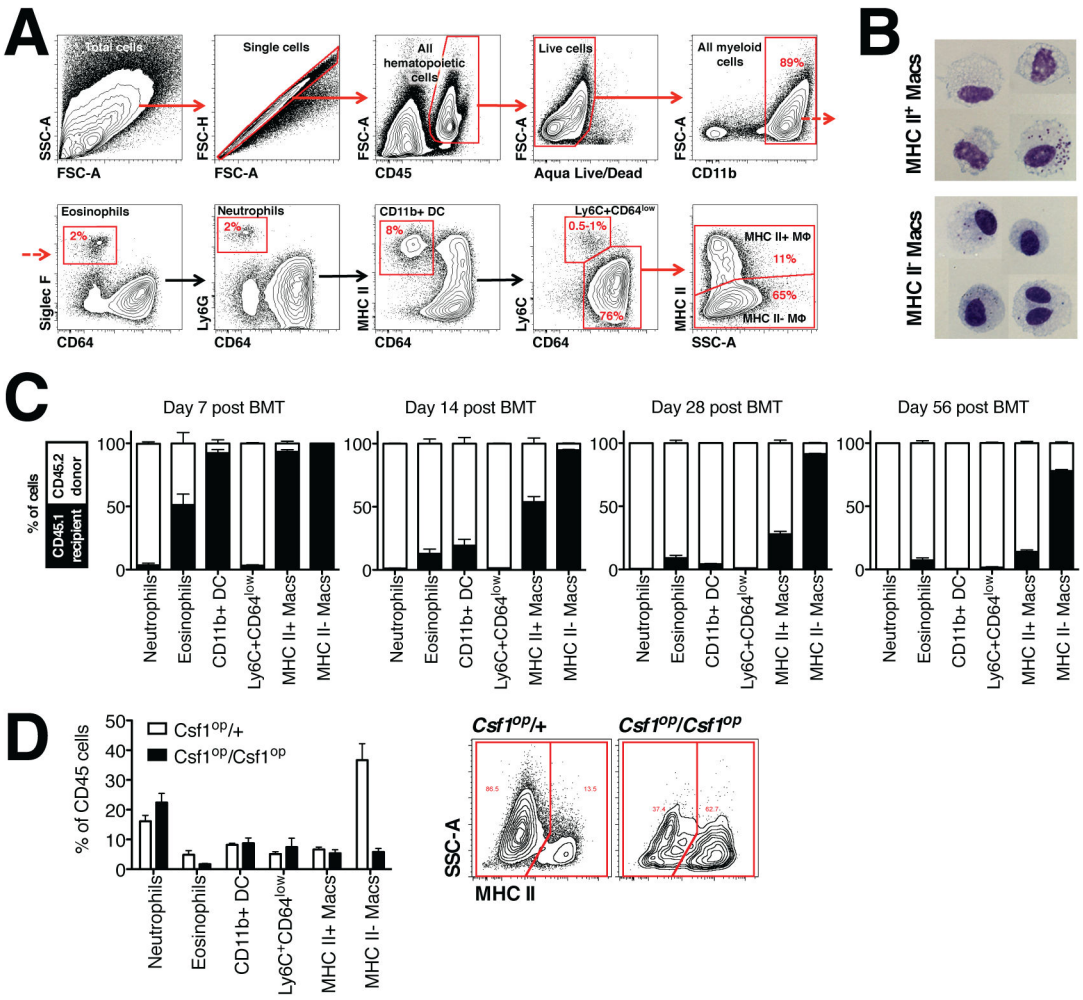

Figure 2. Characterization of synovial macrophages under steady state conditions in the mouse joint

A. Flow cytometry analysis of a mouse joint during steady state conditions. Numbers on the contour plots represent percentages of $CD45^+$ cells. B. Photomicrographs of sorted MHC II^+ and MHC II^- macrophages. Scale bar 5 μm. C. MHC II^- macrophages exhibit radioresistance and do not require input from bone marrow. Bone marrow transfer (n=4 per time point) was performed as described in the Methods. D. Left panel: Number of MHC II^- macrophages was dramatically reduced in the synovium of $Cfs1^{op/op}$ mice (n = 4). Right panel: Representative contour plots showing decrease of MHC II^- macrophages in the synovium. Numbers on the contour plots represent percentages of the parent population (macrophages).

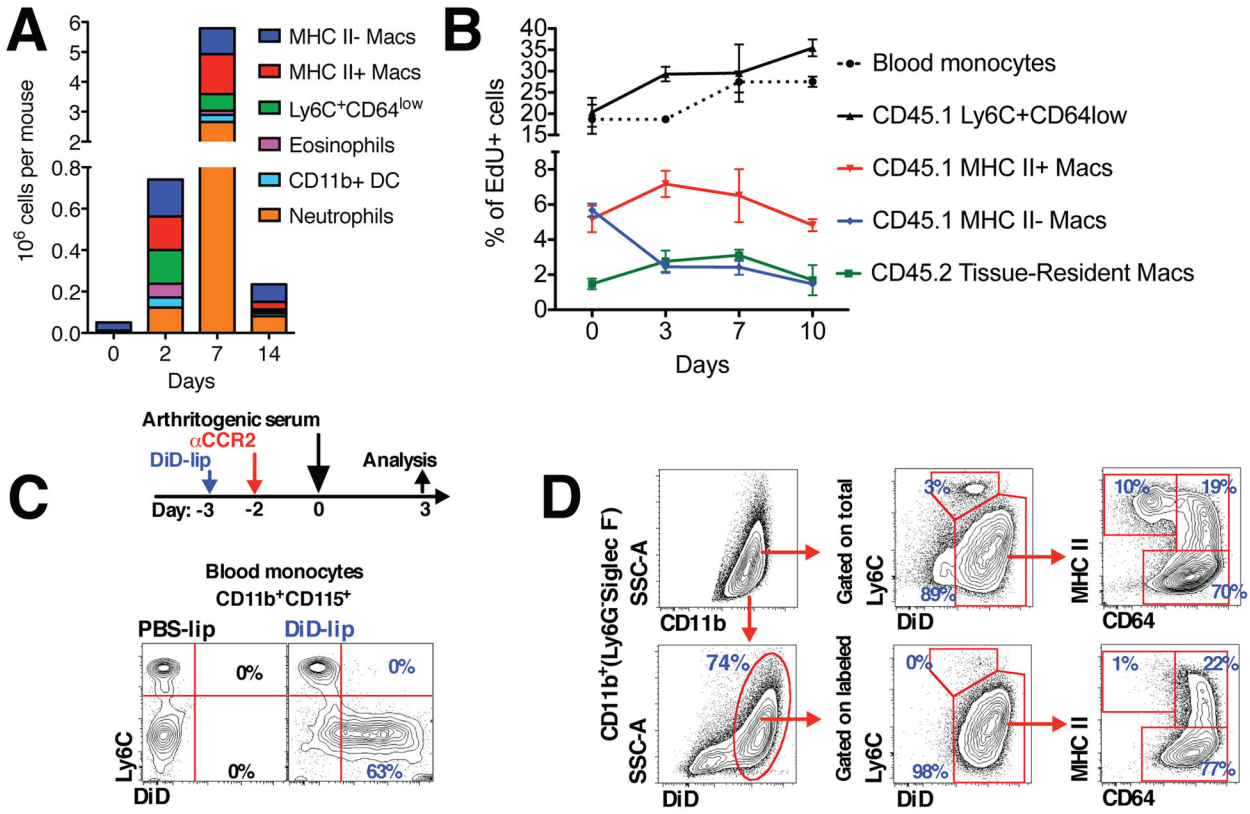

Figure 3. Origin of inflammatory macrophages in the arthritic joint

A. Dynamics of the individual cell subsets in the synovium during the course of STIA (n = 4). B. Analysis of EdU incorporation during the course of STIA. Arthritis was induced in bone marrow chimeras with shielded ankles as described in the Supplemental Methods section. C. Non-classical Ly6C^{-} monocytes were labeled as described in the Methods section. Representative contour plots are shown and numbers represent percentages of monocytes. D. Non-classical Ly6C^{-} monocytes are recruited to the arthritic joint and give rise to both MHC II^{+} and MHC II^{-} macrophages. Data are represented as mean ± SEM.

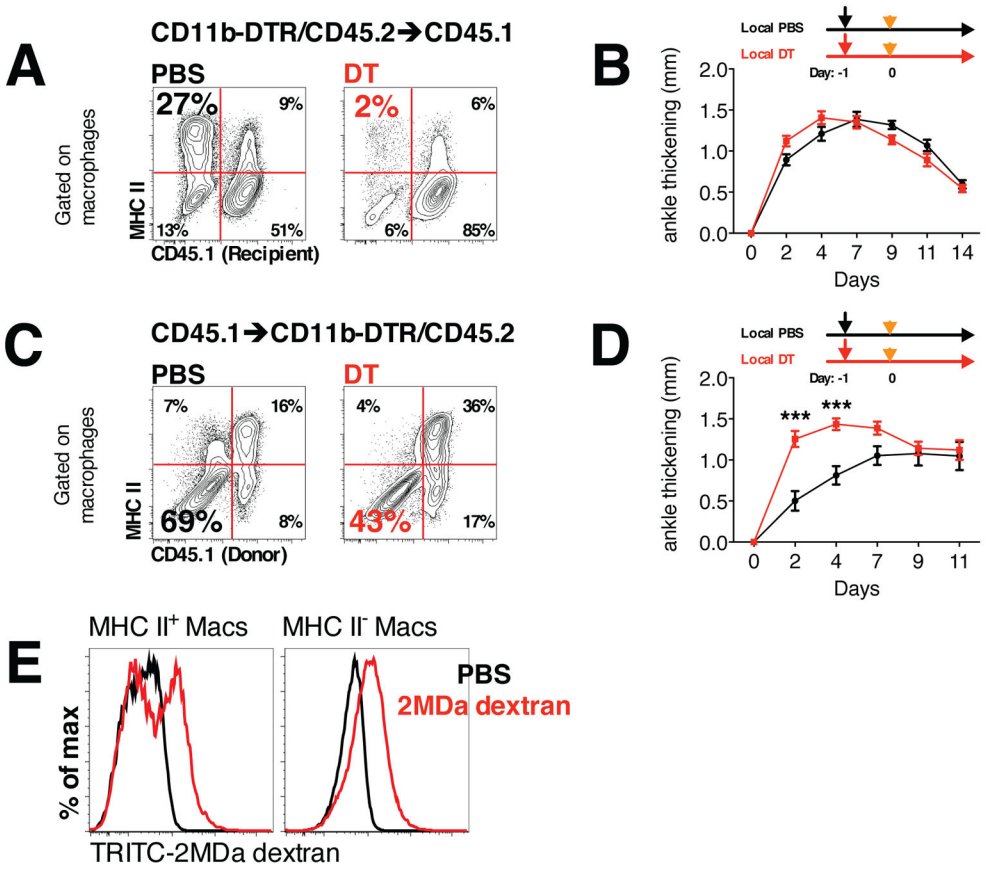

Figure 4. Role of tissue-resident macrophages in the initiation of STIA

A. Local injection of DT depletes donor-derived macrophages in CD11b-DTR→CD45.1 bone marrow chimeric mice. Representative contour plots gated on macrophages are shown (numbers indicate percentages of the parent population). B. Depletion of MHC II^+ macrophages does not affect initiation and development of STIA (n = 5). C. Local injection of DT depletes host macrophages in CD45.1→CD11b-DTR bone marrow chimeric mice and does not affect donor-derived macrophages. Representative contour plots gated on macrophages are shown (numbers indicate percentages of the parent population). D. Depletion of MHC II^- macrophages accelerate development of STIA (n = 10). Data are represented as mean ± SEM. Differences between groups were compared using two-way ANOVA for repeated measurements, with Bonferroni post-test, * $p<0.05$, ** $p<0.01$, *** $p<0.001$. E. Phagocytosis of high molecular weight TRITC-labeled dextran by subpopulations of myeloid cells in the naïve mouse joint. Representative histograms are shown.

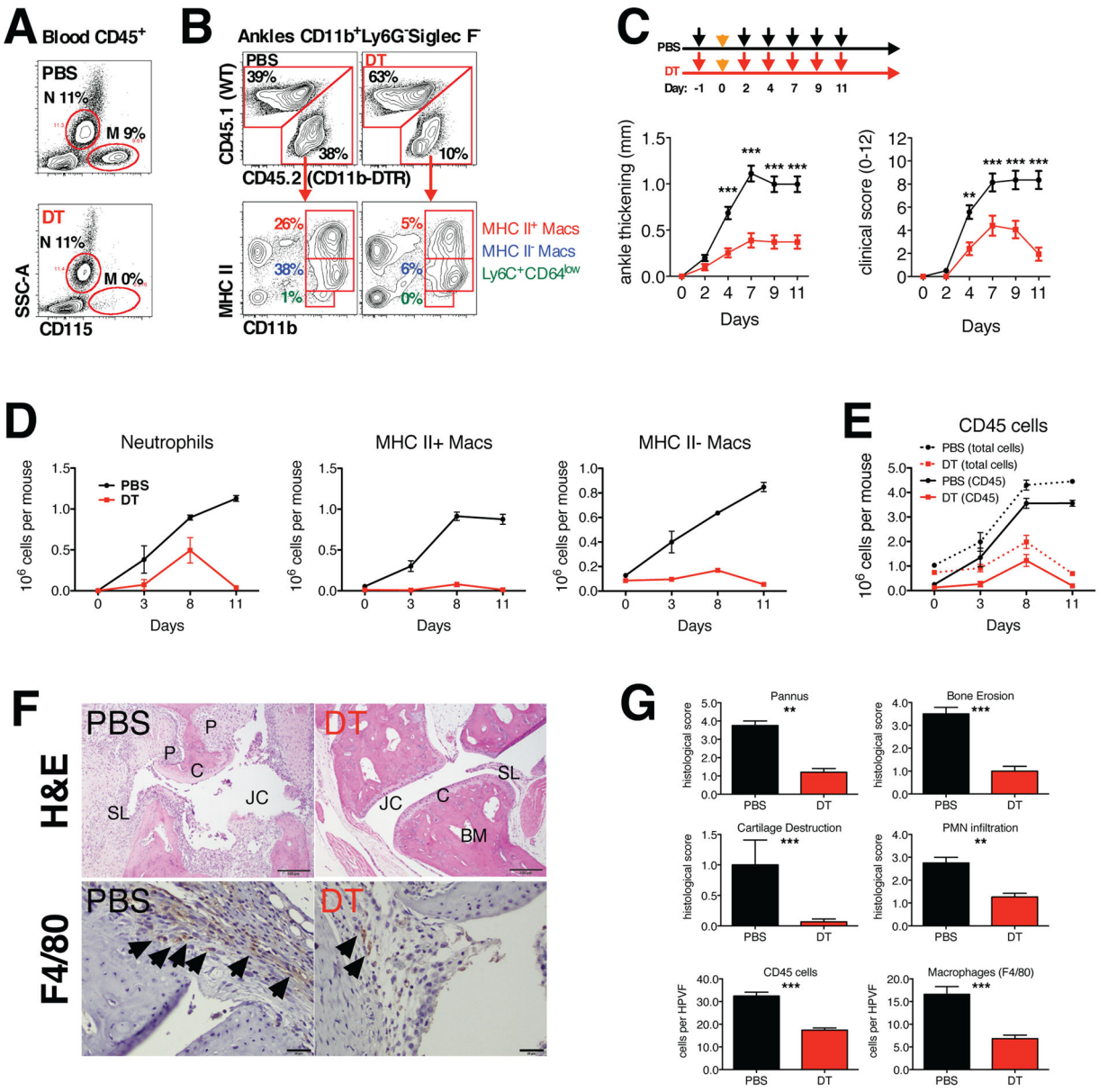

Figure 5. Recruitment of monocytes and differentiation into macrophages are required for development of joint pathology during STIA

A Systemic treatment with DT eliminated blood monocytes while sparing neutrophils. Representative contour plots are shown. Numbers represent percentages of $CD45^+$ cells. B. Systemic treatment with DT eliminates DTR-expressing tissue macrophages (CD45.2) in the synovium of CD11b-DTR(CD45.2)→CD45.1 bone marrow chimeras. Representative contour plots are shown and numbers indicate percentages of $CD45^+$ cells. C. Repeated administration of DT decreases severity of arthritis (n = 10). D. Continuous treatment with DT decreased number of cells recruited to the joint (n=4 per time point). E. Dynamic of myeloid cell subsets in the joints during the course of STIA in PBS and DT-treated mice. F. Depletion of tissue macrophages during effector phase of STIA decreases joint damage. Top panel: hematoxylin and eosin staining (tibiotalar joint is shown), scale bar represents 100

μm. BM – bone marrow, C – cartilage, JC – joint cavity, P – pannus, SL – synovial lining. Bottom panel: immunohistochemical staining for macrophage marker F4/80. Arrows indicate F4/80-positive cells. Scale bar 20 μm. G. Depletion of tissue macrophages decreases histopathological scores. Data are represented as mean ± SEM. Differences between groups were compared using two-way ANOVA for repeated measurements, with Bonferroni post-test, * $p<0.05$, ** $p<0.01$, *** $p<0.001$.

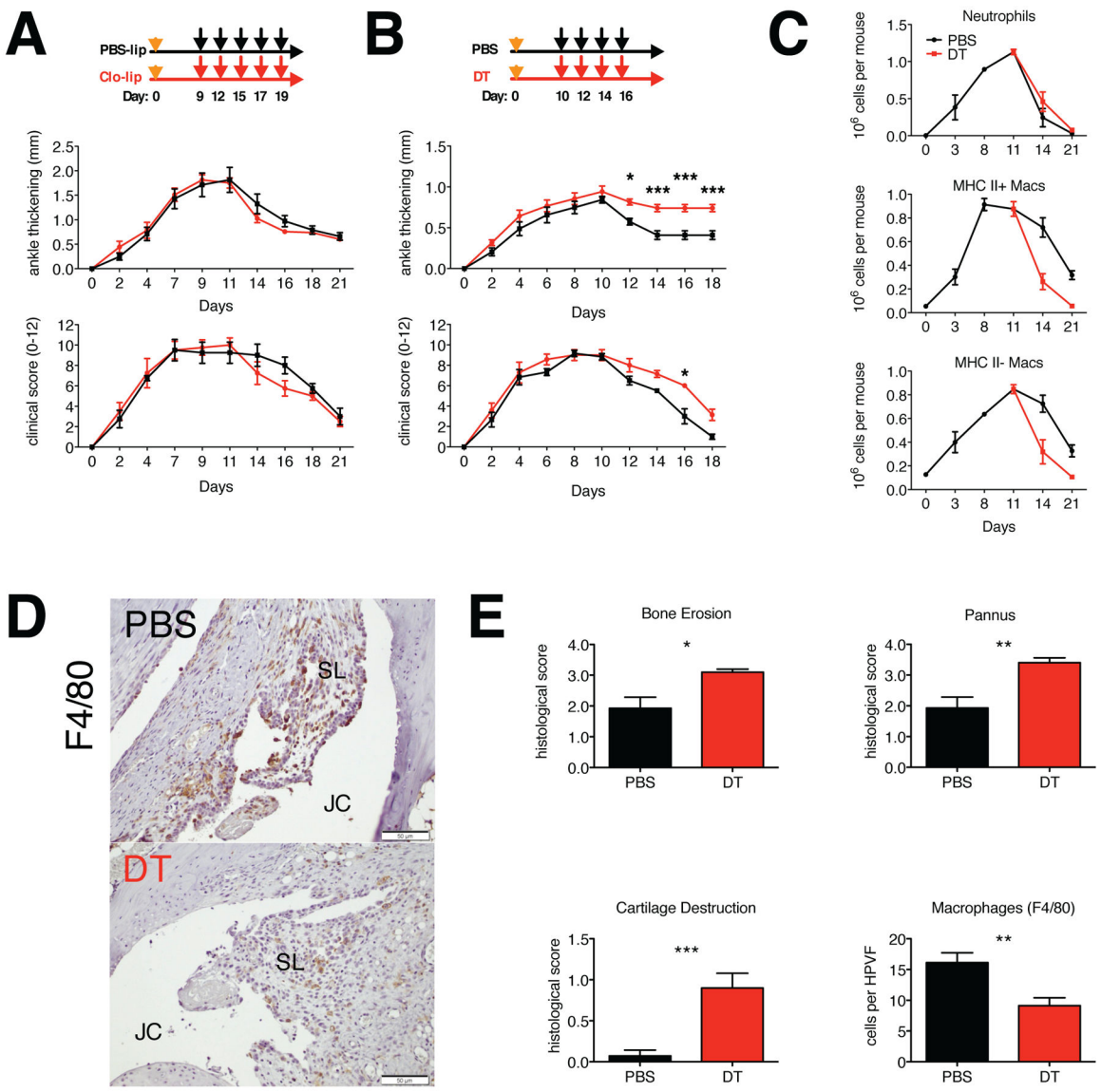

Figure 6. Role of monocytes and macrophages in the resolution of STIA

A. Depletion of monocytes does not affect resolution of STIA (n = 4). B. Depletion of monocytes and tissue macrophages during the resolution phase of STIA delays resolution of arthritis (n = 7). C. Repeated administration of DT depletes tissue macrophages. D. Repeated administration of DT depletes tissue macrophages: Immunohistochemistry was performed on ankle section for F4/80. JC – joint cavity, SL – synovial lining. Scale bar 50 μm. E. Depletion of tissue macrophages during resolution phase results in higher histopathological scores. Data are represented as mean ± SEM. Differences between groups were compared using two-way ANOVA for repeated measurements, with Bonferroni post-test (arthritis), or with Student's t-test (histopathology), * $p<0.05$, ** $p<0.01$, *** $p<0.001$.

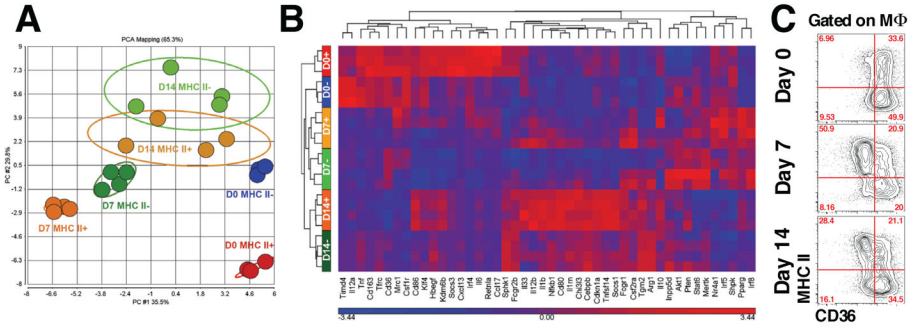

Figure 7. Synovial macrophages switch phenotype during the course of STIA

A. Principal component analysis of gene expression in synovial macrophages confirms the differential origins of MHC II^+ and MHC II^- synovial macrophages in the steady state. B. Hierarchical clustering of 46 genes differentially expressed across the dataset (FDR q-value < 0.001). C. Expression of CD36 on synovial macrophages during the course of STIA and analyzed by flow cytometry. Representative contour plots are shown. Numbers represent percentages of the parent gate.